UWB monocycle pulse generation using two-photon absorption in a silicon waveguide

Yang Yue,[1,*] Hao Huang,[1] Lin Zhang,[1] Jian Wang,[1] Jeng-Yuan Yang,[1] Omer F. Yilmaz,[1] Jacob S. Levy,[2] Michal Lipson,[2] and Alan E. Willner[1]

[1]Department of Electrical Engineering, University of Southern California, Los Angeles, California 90089, USA

[2]School of Electrical and Computer Engineering, Cornell University, Ithaca, New York 14853, USA

*Corresponding author: yyue@usc.edu

Received December 20, 2011; revised December 20, 2011; accepted December 21, 2011; posted December 21, 2011 (Doc. ID 152762); published February 8, 2012

We propose and experimentally demonstrate ultrawideband monocycle pulse generation using nondegenerate two-photon absorption in a silicon waveguide. The free-carrier absorption induced pulse tail at the rising edge of inverted probe pulse is largely compensated by the overlapped pump pulse and results in a symmetric negative monocycle pulse. A 143 ps Gaussian monocycle pulse is successfully obtained with a 131.7% fractional 10 dB bandwidth using a 68 ps pulsed pump. The 10 dB bandwidth and center frequency of the RF spectrum for the generated monocycle pulse can be largely tuned using an optical delay line. An operational bandwidth of 30 nm is demonstrated experimentally with stable performance, and larger optical bandwidth is expected.

OCIS codes: 060.5625, 130.4310, 230.7370, 350.4010.

In general, ultrawideband (UWB) signals have garnered much interest over the past several years for their ability to encode high-capacity, broadband data on monocycle pulses [1]. This has certainly been true in the electronic domain, and the interest has spilled over into trying to use optics to efficiently generate UWB pulses for use in microwave and RF photonics applications. Optically generating UWB pulses has many advantages, such as high speed, large tunability, and immunity to electromagnetic interference [2]. Several optical techniques have been developed for generating UWB pulses, including: (a) phase to intensity modulation conversion [3], (b) photonic microwave delay line filter [4], and (c) spectral shaping and dispersion-induced frequency-to-time mapping [5]. It is highly desirable to make the system compact and even realize on-chip integration. Some integrated schemes based on cross-absorption modulation in semiconductor optical amplifier and electroabsorption modulator have been demonstrated for UWB pulse generation [6,7]. However, these schemes used complex amplifier or modulator with III-V materials. A laudable goal would be to generate UWB pulses on the silicon complementary metal–oxide–semiconductor (CMOS) platform with simplified structure.

Recently, silicon photonics has attracted a lot of attention due to its great potential for CMOS compatibility [8]. The bandgap of silicon crystal is around 1.11 eV. This brings silicon into the 1.1 to 2.2 μm broad two-photon absorption (TPA) wavelength range, which covers the widely used telecom band [9]. Degenerate or nondegenerate TPA is a process that simultaneously absorbs two photons of identical or different frequencies in order to excite a molecule from a lower energy state to a higher energy state. As an ultrafast absorption effect, TPA has been used for optical switching, logic gates, and pulse compression in silicon waveguides (Si WGs) [10–12].

In this Letter, we propose and experimentally demonstrate UWB monocycle pulse generation using nondegenerate TPA in a Si WG. A pulsed pump in the Si WG inversely modulated the continuous-wave (CW) probe during the nondegenerate TPA process. The monocycle pulse is optically generated after combining the inversely modulated probe and pulsed pump in the time domain. Using a pulsed pump with a 68 ps full width at half-maximum (FWHM), a UWB monocycle pulse with a 143 ps pulse width is generated with a 131.7% fractional bandwidth. The proposed TPA-based UWB monocycle pulse generation scheme also shows large tunability and the potential for broadband operation.

A conceptual diagram of all-optical UWB monocycle pulse generation using nondegenerate TPA in a Si WG is shown in Fig. 1. A CW probe and a pulsed pump are aligned to the Si WG's TE-like mode and coupled together. After passing through the WG, the CW probe is inversely modulated by the pulsed pump during the nondegenerate TPA process in the Si WG. By properly controlling the relative delay and power relationship between the attenuated pump and the inversely modulated probe, positive and negative UWB monocycle pulses with different shapes can be generated in the optical domain after their recombination.

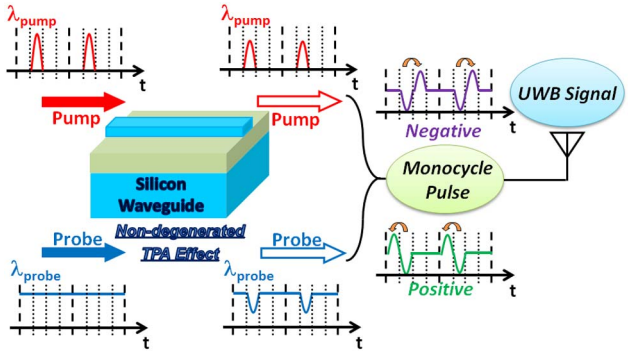

Fig. 1. (Color online) Concept diagram of silicon waveguide-based UWB monocycle pulse generation using nondegenerated two-photon absorption effect.

The experimental block diagram of our setup is shown in Fig. 2. A CW laser at $\lambda_{\text{pump}} = 1550.4$ nm is first modulated by a Mach–Zehnder modulator (MZM) with 40 Gbit/s non-return-to-zero amplitude modulation. The pattern generator is programmed to provide a 200 bit iterative pattern, which corresponds to a 200 MHz repetition rate. The pattern has only a few consecutive "1"s, while the others are all "0"s. By setting the number of "1"s from 1 to 5, we can obtain electrical pulses with variable pulse width from 25 to 125 ps. First, the pulsed pump is boosted to 13.8 dBm using an erbium-doped fiber amplifier (EDFA). Its 90% power port is attenuated by a variable optical attenuator (VOA1), and then combined with a 10 dBm CW probe at $\lambda_{\text{probe}} = 1569.6$ nm and feeds into the Si WG. In this experiment, a 4.046 cm long waveguide with a 776×300 nm^2 cross section is used. Lensed fibers with 2.5 μm spot diameter (as shown in the inset of Fig. 2) are used to couple the light into and out of the waveguide. The total insertion loss is ~16.2 dB and the waveguide propagation loss is estimated to be ~2 dB/cm. By aligning both the pump and probe light polarizations to the TE-like mode of the Si WG, the maximum TPA modulation efficiency (~80%) can be achieved with a 26 ps pump pulse. In the inset waveform "modulated probe", we can see the long tail (at the rising edge of the inversely modulated probe) generated by the free-carrier absorption (FCA). From the output of the Si WG, we filtered out the inversely modulated probe using a 2 nm bandpass filter (BPF). The left 10% pulse pump after optical coupler (OC1) is then recombined with the modulated probe through OC3. Using a tunable optical delay line (ODL) and VOA2, the relative time delay and amplitude relationship between the pump and the inversely modulated probe are well controlled. Then, the generated UWB monocycle pulse is converted to an electrical signal with a 40 GHz photodetector for the electrical spectrum analyzer (ESA) and the oscilloscope (Scope). Also, an optical spectrum analyzer (OSA) is used after OC3 to monitor the optical spectrum.

To obtain a desirable UWB monocycle signal, it is of great importance to increase the modulation depth of the nondegenerate TPA. Previous research has shown that >90% modulation depth can be achieved using TPA in a Si WG with a 1.6 ps pump pulse with very low energy [11]. Here, we first study the modulation efficiency of the waveguide in our experiment. By keeping the power of the CW probe at 10 dBm, we increase the pump power to reach ~15 dBm total input power to the Si WG. From that point, we gradually reduce the pump power into the Si WG using VOA1 and study its impact on the TPA, as shown by the B-Spline curves in Fig. 3. The probe modulation depth shows a significant reduction. For the pump pulse with a 26 ps FWHM, the probe modulation depth decreases from 79.4% to 26.1% as the pump pulse peak power decreases from 883.8 to 51.8 mW. From Fig. 3(a), we can see that, at a fixed total input power (rightmost points of the curves), the pump with a larger pulse width exhibits a smaller probe modulation depth because of the less peak power. With a 15 dBm total input power into the WG, the probe modulation depths of $\text{FWHM}_{\text{pump}} = 26$ and 119 ps are 79.4% and 47.9%, respectively. The FWHM of the modulated probe pulse is relatively stable over pump power, as shown in Fig. 3(b). The small increase of the $\text{FWHM}_{\text{probe}}$ is mainly due to the enhanced FCA induced by the increased pump power.

To generate UWB monocycle pulses, we choose the $\text{FWHM}_{\text{pump}}$ as 45, 68, and 93 ps, respectively. The peak powers of the pump and the probe are kept close to each other, providing a monocycle pulse that has relatively symmetric amplitude. For a positive monocycle pulse (the pump pulse right ahead of the inversely modulated probe pulse in the time domain), the FCA-generated tail at the rising edge of the inverted probe pulse results in an asymmetric monocycle pulse and affects the shape of the RF spectrum. By generating a negative monocycle pulse, the FCA-induced pulse tail is largely compensated by the overlapped pump pulse and produces a symmetric monocycle pulse. From Fig. 4(a)–(c) we can see that, 45 ps pump has the largest modulation depth, and thus a larger monocycle pulse amplitude. While the total power of the monocycle pulse is close for input pump with different FWHM, thus the electrical power spectra are of the similar level. As shown in Fig. 4(b), the UWB monocycle pulse generated from a 68 ps pulsed pump has a 143 ps pulse width. The spectrum of the generated monocycle

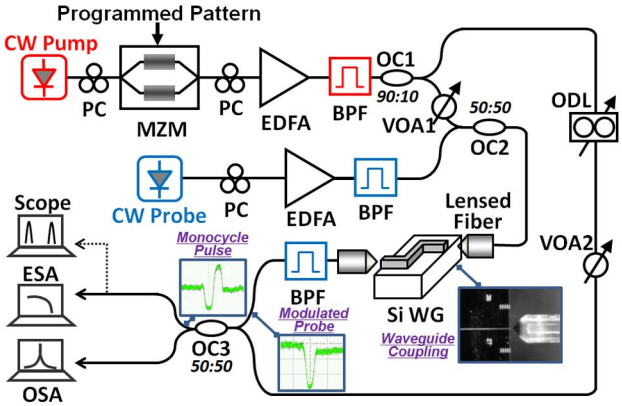

Fig. 2. (Color online) Experimental setup. Pulsed pump and CW probe are coupled to Si WG. The inversely modulated probe then combines with the pump to generate monocycle pulses.

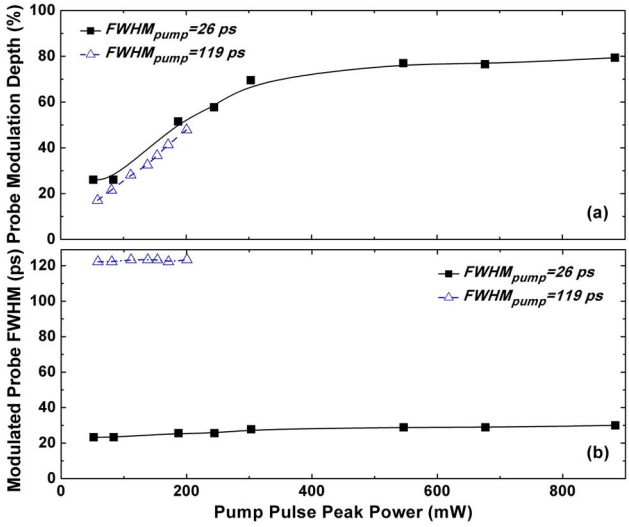

Fig. 3. (Color online) Effects of nondegenerated two-photon absorption. (a) Probe modulation depth, and (b) modulated probe FWHM as a function of pump pulse peak power for different pump pulse width.

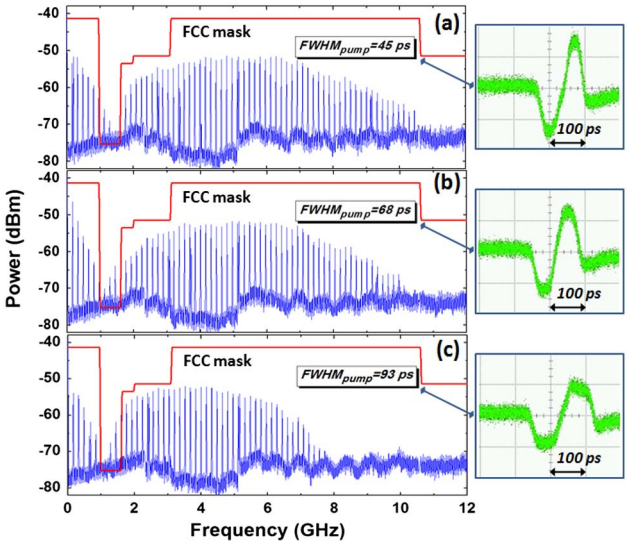

Fig. 4. (Color online) Ultrawideband signal generation. RF power spectra of generated monocycle pulse with (a) $\mathrm{FWHM_{pump}} = 45$ ps, (b) 68 ps, and (c) 93 ps.

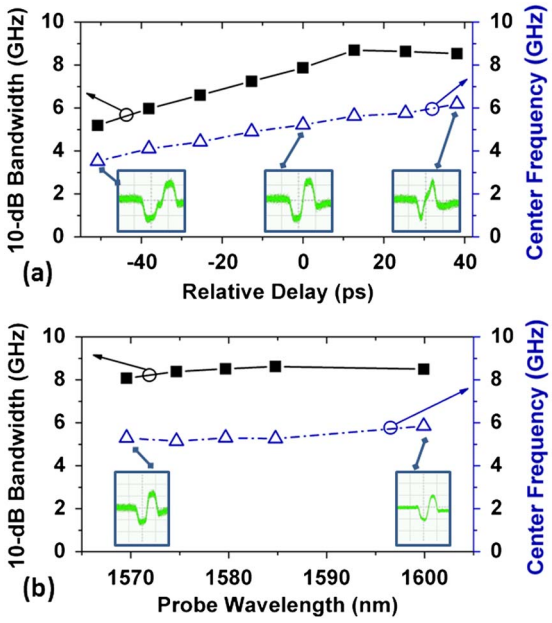

Fig. 5. (Color online) 10 dB bandwidth and center frequency of the RF spectrum as a function of (a) relative delay between the pump and inversely modulated probe ($\mathrm{FWHM_{pump}} = 68$ ps); (b) probe wavelength ($\mathrm{FWHM_{pump}} = 68$ ps, $\lambda_{\mathrm{pump}} = 1550.4$ nm).

pulse is measured by an ESA. It can be seen that the electrical spectrum has a central frequency of 5.62 GHz with a 10 dB bandwidth of 7.4 GHz, from 1.92 to 9.32 GHz. The fractional bandwidth is 131.7%, which meets the Federal Communications Commission requirement of 20%. From Fig. 4 we can see that the bandwidth of the electrical spectrum is inversely proportional to the monocycle pulse width. A pump pulse with 93 ps FWHM provides a monocycle pulse with 6.11 GHz 10 dB RF bandwidth.

The relative delay of the pump pulse and the inversely modulated probe can be controlled using the ODL in the experimental setup. By tuning the ODL, the width and shape of the generated monocycle pulse can be controlled properly. As shown in Fig. 5(a), this provides the ability to tune the bandwidth and the center frequency of the RF spectrum for the generated UWB signal. A maximal 10 dB bandwidth can be achieved with a proper delay. Also, the center frequency can be tuned from 4 to 6 GHz. In addition, the 10 dB bandwidth and center frequency of the RF spectrum can be tuned by controlling the FWHM and the power of the pump pulse.

To take advantage of the ultrahigh bandwidth in the optical domain, broadening the operational wavelength range of the UWB pulses is of great importance, especially for point-to-multipoint multicasting or multiuser UWB system [13]. Wavelength conversions over 200 nm have been demonstrated using TPA in an Si WG [14]. This paves the way for on-chip broadband applications using nondegenerate TPA. As shown in Fig. 5(b), we vary the probe wavelength from 1570 to 1600 nm while only changing the passing window of the filters. The 10 dB bandwidth and center frequency of the RF spectrum are relatively stable across a 30 nm optical bandwidth.

The asymmetry of positive and negative monocycle pulses due to the FCA may limit the application of pulse polarity modulation. There are potentially two alternative ways to implement data modulation on the proposed monocycle pulse generation scheme. One straightforward way is to encode data to the time location of the pump pulse for pulse position modulation. Second, it is also possible to modulate the UWB monocycle pulse with on–off keying by using an extra optical switch.

We acknowledge the support of the National Science Foundation (NSF)-funded Center for the Integrated Access Networks (CIAN).

References

1. D. Porcino and W. Hirt, IEEE Commun. Mag. **41**, 66 (2003).
2. J. P. Yao, F. Zeng, and Q. Wang, J. Lightwave Technol. **25**, 3219 (2007).
3. F. Zeng and J. P. Yao, IEEE Photon. Technol. Lett. **18**, 823 (2006).
4. Q. Wang and J. P. Yao, Opt. Express **15**, 14667 (2007).
5. C. Wang, F. Zeng, and J. P. Yao, IEEE Photon. Technol. Lett. **19**, 137 (2007).
6. Q. Wang, F. Zeng, S. Blais, and J. Yao, Opt. Lett. **31**, 3083 (2006).
7. T.-H. Wu, J.-p. Wu, and Y.-J. Chiu, Opt. Express **18**, 3379 (2010).
8. M. Hochberg and T. Baehr-Jones, Nat. Photon. **4**, 492 (2010).
9. Q. Lin, O. J. Painter, and G. P. Agrawal, Opt. Express **15**, 16604 (2007).
10. T. K. Liang, L. R. Nunes, T. Sakamoto, K. Sasagawa, T. Kawanishi, M. Tsuchiya, G. R. A. Priem, D. Van Thourhout, P. Dumon, R. Baets, and H. K. Tsang, Opt. Express **13**, 7298 (2005).
11. T. K. Liang, L. R. Nunes, M. Tsuchiya, K. S. Abedin, T. Miyazaki, D. Van Thourhout, W. Bogaerts, P. Dumon, R. Baets, and H. K. Tsang, Opt. Commun. **265**, 171 (2006).
12. E.-K. Tien, N. S. Yuksek, F. Qian, and O. Boyraz, Opt. Express **15**, 6500 (2007).
13. T. Huang, J. Li, J. Sun, and L. R. Chen, Opt. Express **19**, 15885 (2011).
14. H. Fukuda, K. Yamada, T. Tsuchizawa, T. Watanabe, H. Shinojima, and S. Itabashi, in *Integrated Photonics Research and Applications/Nanophotonics*, OSA Technical Digest Series (Optical Society of America, 2006), paper ITuH1.